J Mater Sci (2009) 44:5760–5767
DOI 10.1007/s10853-009-3807-y

Effect of iron on the electrical properties of lead–bismuth glasses

Shaaban M. Salem

Received: 13 April 2009 / Accepted: 12 August 2009 / Published online: 27 August 2009

Abstract Semiconducting oxide glasses of the system $(80 - x)Bi_2O_3$–$20PbO$–xFe_2O_3, where $x = 5$, 10 and 15 mol.%, were prepared and investigated for dielectric properties in the frequency range 120–100 KHz and temperature range 300–550 K. Analysis of the electrical properties has been made in the light of small polaron hopping model. The parameters obtained from the fits of the experimental data to this model are reasonable and consistent with glass composition. The conduction is attributed to non-adiabatic hopping of small polaron. The ac conductivity results suggest that the correlated barrier hopping (CBH) is dominant in ac conductivity.

Introduction

Iron bismuthate glasses are electronically conducting glasses with polaronic conduction mechanism [1–6]. In these glasses, iron ions exist in two valence states and the electrical conduction occurs by hopping of polaron from Fe^{2+} to Fe^{3+}. In hopping process, the electron disorders its surroundings, by moving its neighboring atoms from their equilibrium positions causing structural defects in the glass network named small polarons. Hence, small polarons are charge carriers trapped by self-induced lattice distortions, which transport consists of phonon-assisted hopping.

It was also reported that the glasses containing bismuth oxide exhibit the high refractive index, IR transmission, and nonlinear optical susceptibilities [7–10]. The large polarizability of bismuth in oxide glasses makes them suitable for optical devices and environmental guidelines. However, bismuth oxide is not a traditional glass former and cannot form glass by itself. In the presence of strong polarizing cations, Bi^{3+} ions can reduce its coordination number from six to three and the glass networks may consist of both $[BiO_6]$ highly distorted octahedral and $[BiO_3]$ pyramidal units [11, 12]. Due to its dual role, as modifier with $[BiO_6]$ octahedral and as glass former with $[BiO_3]$ pyramidal units, bismuth ions may influence the electrical properties of glasses.

The aim of this work was, thus, to perform measurements of dielectric constant of the glass system of the composition $(80 - x)Bi_2O_3$–$20PbO$–xFe_2O_3, where $x = 5$, 10 and 15 mol.%, at the temperature range 300–600 K and in the frequency range from 120–100 KHz, in order to investigate the response of the permanent dipoles as a function of frequency, temperature, and glass composition. The dc and ac electrical conductivity investigated of the glass system to understand the mechanism of electrical conduction. The density of these systems with different molar percentages of Fe_2O_3 was also measured to understand whether chemical reaction had taken place or not on the introduction of Fe_2O_3 in the Bi_2O_3–PbO glass.

Experimental

Glass samples were prepared from the reagent grade chemicals Bi_2O_3, PbO, and Fe_2O_3 (99.9%). The chemicals with appropriate properties (Table 1) were mixed uniformly. The homogeneous mixture was taken in a platinum crucible and placed in a furnace. The mixture was melted in the temperature range 1,100–1,150 °C depending on the compositions for 1 h. The melt was then poured on a thick copper block and immediately quenched by pressing with

S. M. Salem (✉)
Department of Physics, Faculty of Science, Al Azhar University, Nasr City, Cairo 11884, Egypt
e-mail: shaabansalem@gmail.com

Table 1 Chemical composition and physical properties of Bi_2O_3–PbO–Fe_2O_3 glasses

Glass no.	Composition (mol.%)			d (g cm^{-3})	$N \times 10^{21}$ (cm^{-3})	R (Å)	θ_D (K)	W (eV)
	Bi_2O_3	PbO	Fe_2O_3					
1	75	20	5	4.96	2.674	7.204	729	0.950
2	70	20	10	4.87	5.252	5.752	716	0.895
3	65	20	15	4.78	7.732	5.056	711	0.821

another similar copper block. X-ray powder diffraction (XRD) measurements have been carried out on Shimadzu XD-DI, X-ray Diffractometer VG 207RII and Cu K_α = 1.54056 Å for grounded powder of the as-quenched samples as a necessary technique for proving the amorphous nature of the samples. The density of the samples was measured at room temperature by Archimedes principle using carbon tetrachloride as an immersion liquid. The concentration of iron ion, N (cm^{-3}), was estimated using $N = dPN_A/(A_w \times 100)$, where d is the density of the sample, P the weight percentage of atoms, N_A the Avogadro constant, and A_w the atomic weight.

The dc electrical conductivity was measured by means of two-probe method, which was appropriate for high resistance materials. Silver painted electrodes were pasted on the polished surface of the samples, then were situated between two polished and cleaned copper electrodes. The current is monitored by means of an electrometer [model: 425A HP], milivoltmeter for measuring the temperature over temperature range 300–550 K with heating rate 2 K/min, constant voltage source 24 V, and a home-made furnace. Isothermal ac measurements were done using a computer controlled CRL bridge (Stanford Res. Model SR-720), for measurements in the frequency range 0.12–100 kHz and temperature range 300–550 K. The calculation of the conductivity $\sigma(\omega)$ and relative permittivity $\varepsilon(\omega)$ were performed separately using the experimental data and dimensions of the samples. All experimental data at a given temperature is contained in $G(\omega)$ and $C(\omega)$, where G is the conductance, C the capacitance and $\omega = 2\pi f$ the angular frequency. The conductivity, σ, and relative permittivity, ε, were σ calculated from the impedance measurements using the equations $\sigma = Gl/A$ and $\varepsilon = Cl/\varepsilon_o A$, where A and l are the sample area and thickness, respectively, ε_o the permittivity of free space.

Results and discussion

The glassy state was confirmed by the absence of peaks in XRD patterns. The XRD patterns exhibit a broad diffuse scattering at low angles instead of crystalline peaks, confirming a long-range structural disorder characteristic of amorphous network. The densities of the glasses are shown in Fig. 1, which decreased with increasing Fe_2O_3 content.

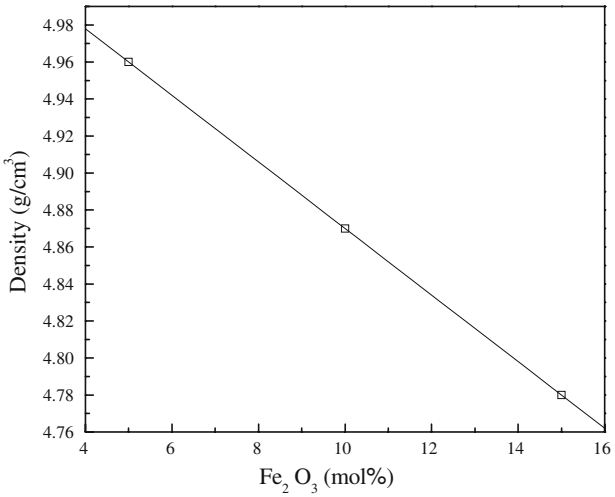

Fig. 1 Effect of Fe_2O_3 content on density (d) for different glass compositions

These were found to be of the same order when compared with those of bismuthate glasses [13, 14]. These trends can be explained rather simply as to the replacement of a lighter cation (Fe) by heavier one (Bi) [14].

Figure 2 shows the variation of logarithm of dc conductivity of Bi_2O_3–PbO–Fe_2O_3 glasses as a function of inverse temperature (T). It is observed that σ increases smoothly with increasing temperature, indicating temperature-dependent activation energy, W, characteristic of small polaron hopping (SPH) conduction mechanism in TMO glasses [7, 9]. At high temperature ($T > \theta_D/2$, where θ_D is the Debye temperature), the conductivity data of the Bi_2O_3–PbO–Fe_2O_3 glasses can be interpreted in terms of the phonon-assisted hopping model given by Mott and Davis [15, 16] namely

$$\sigma = \frac{v_o N e^2 R^2}{kT} C(1-C)\exp(-2\alpha R)\exp\left(\frac{-W}{kT}\right) = \frac{\sigma_o}{T}\exp\left(\frac{-W}{kT}\right), \quad (1)$$

$$\sigma_o = \frac{v_o N e^2 R^2}{kT} C(1-C)\exp(-2\alpha R), \quad (2)$$

where σ_o is the pre-exponential factor depending on the separation between the conduction carriers, v_o the longitudinal optical phonon frequency ($\sim 10^{13}$ Hz), α the inverse localization length of the s-like wave function

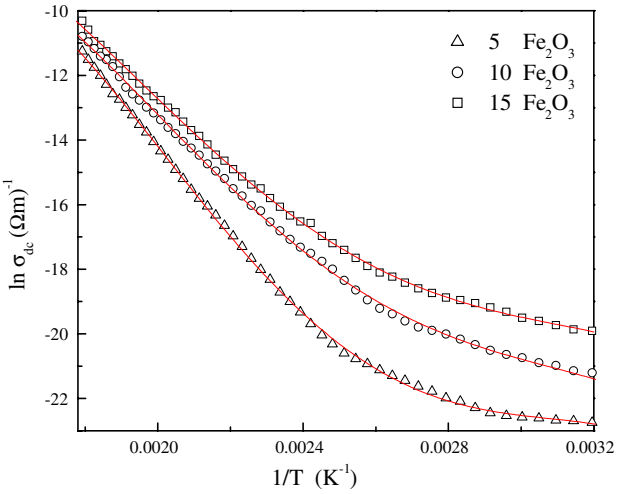

Fig. 2 Temperature dependence of dc conductivity (ln σ_{dc}) for different glass compositions

assumed to describe the localized state at each site, ($C = Fe^{2+}/\sum Fe$) the ratio of concentration of TMI (transition metal ions) in the low valence state to the total concentration of the TMI, R the average hopping distance $(=1/N)^{1/3}$, W the activation energy, e the electronic charge, K the Boltzmann constant, and T absolute temperature. The experimental conductivity data above a typical temperature ($T < \theta_D/2$), where nonlinearity is observed in Fig. 2, are fitted with Eq. 1 by least-squares method and the best fit parameters are shown in Table 2. The small polaron hopping model predicts an appreciable departure from the linear curve of log σ against $1/T$ at a temperature $\theta_D/2$, where θ_D (Debye temperature) is defined by the relation $h\nu_o = k\theta_D$. Assuming a strong electron–phonon interaction, Austin and Mott [16] showed that the activation energy W is the result of polaron formation of binding energy W_p, and an energy difference W_D, which might exist between the initial and final sites due to variation in the local arrangements of ions, i.e.

$$W = W_H + W_D/2 \quad \text{for } T > \frac{\theta_D}{2}, \tag{3}$$

$$W = W_D \quad \text{for } T < \frac{\theta_D}{4}, \tag{4}$$

where W_H is the polaron hopping energy and W_D the disorder energy arising from the energy difference of the neighbors between two hopping sites. The nature of polaron hopping mechanism (adiabatic or non-adiabatic) can be estimated [17, 18] from a plot of logarithm of the conductivity against activation energy at different experimental temperatures (T) for all these glasses. It is expected that the hopping will be in the adiabatic regime if the temperature estimated (T_e) from the slope of such a plot is close to the experimental temperature, otherwise the hopping will be in the non-adiabatic regime. In this way, hopping at higher temperatures is inferred to be in the adiabatic regime for the vanadate glasses with conventional glass formers [19, 20]. From the plot of log σ against W at different temperatures for Bi_2O_3–PbO–Fe_2O_3 glasses (Fig. 3), the estimated temperatures (shown within parenthesis) obtained from the slopes are quite different from the experimental temperature (shown outside the parenthesis) suggesting non-adiabatic hopping conduction mechanism for the Bi_2O_3–PbO–Fe_2O_3 glasses. This non-adiabatic conduction mechanism is further confirmed from the calculation of the polaron bandwidth (J) from the following relation [21]:

$$J > \left(\frac{2kTW_H}{\pi}\right)^{1/4}\left(\frac{\hbar\nu_o}{\pi}\right)^{1/2} \text{(Adiabatic hopping)}, \tag{5}$$

$$J < \left(\frac{2kTW_H}{\pi}\right)^{1/4}\left(\frac{\hbar\nu_o}{\pi}\right)^{1/2} \text{(Non}-\text{adiabatic hopping)}, \tag{6}$$

where J is the polaron bandwidth related to the electron wave function overlap on the adjacent sites. The values of $(2kTW_H/\pi)^{1/4}(\hbar\nu_o/\pi)^{1/2}$ varies from 0.036 to 0.043 eV at 300 K for all the glass concentrations. The values of J independently estimated from the relation [21], $J \approx e^3[N(E_F)/(\varepsilon_o\varepsilon_p)^3]^{1/2}$, varied from 0.16×10^{-4} to 4.03×10^{-4} eV depending on the concentration. These values of J are much smaller than those estimated from the right-hand side of Eq. 6 confirming non-adiabatic hopping conduction for these glasses. Holstein [21] has suggested a method for calculating the polaron hopping energy W_H:

$$W_H = (1/4N)\sum\nolimits_p [\gamma_p]^2\hbar\omega_q \cong \frac{W_p}{2} = \frac{e^2}{4\varepsilon_p}\left(\frac{1}{r_p} - \frac{1}{R}\right), \tag{7}$$

where W_p is the polaron binding energy and $(1/\varepsilon_p) = (1/\varepsilon_\infty) - (1/\varepsilon_o)$, and ε_o and ε_∞ are the static and high-frequency dielectric constant of the glass, respectively. Using W_H, r_p, and R values, we estimated $\varepsilon_p = 35.01$–5.59

Table 2 Physical properties and polaron hopping parameters of Bi_2O_3–PbO–Fe_2O_3 glasses

Glass no.	$\nu_o \times 10^{13}$ (S^{-1})	W_H (eV)	r_p (Å)	ε_p	$N(E_F) \times 10^{21}$ ($eV^{-1}m^{-3}$)	γ_p
1	1.521	0.459	2.902	13.26	0.806	17.44
2	1.494	0.474	2.318	19.23	1.639	15.33
3	1.483	0.287	2.037	36.12	2.502	9.357

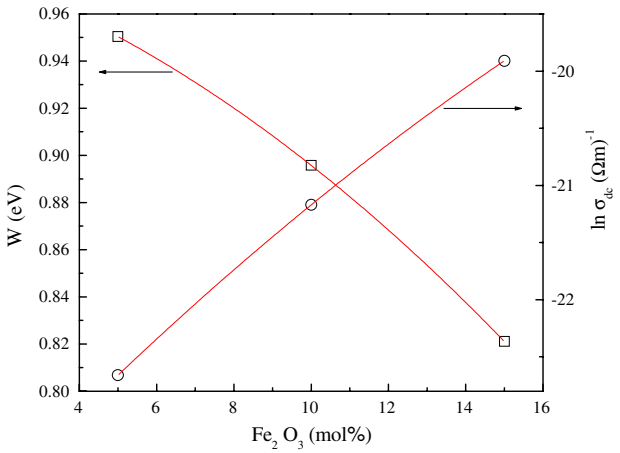

Fig. 3 Effect of Fe_2O_3 content on dc conductivity (ln σ_{dc}) at $T = 300$ K and activation energy (W) for different glass compositions

(Table 2) for $Fe_2O_3 = 5$–15 mol.%, which were comparable to those for Fe_2O_3–Bi_2O_3–$K_2B_4O_7$ glasses ($\varepsilon_p = 27.4$–43.0) [22], γ_p is the electron–phonon coupling constant and ω_q the frequency of the optical phonons of wave number. Using the mean spacing between the transition metal ions R calculated from the glass density data, the polaron radius is estimated by Bogomolov et al. [23], and they have calculated the polaron radius r_p for a non-dispersive system of frequency v_o for the estimated values of r_p:

$$r_p = 1/2(\pi/6N)^{1/3} = \frac{R}{2}\left(\frac{\Pi}{6}\right)^{1/3}. \quad (8)$$

The possible effect of disorder has been neglected in the above calculation; the small values of polaron radii suggest that the polarons are highly localized [23]. The density of states at the Fermi level can be estimated from the following expression [15]:

$$N(E_F) = 3/4\pi R^3 W. \quad (9)$$

The results for the present glasses are listed in Table 2. The values of $N(E_F)$ are reasonable for localized states. We estimate the optical phonon frequency, (v_o) in Eq. 2 using the experimental data from Table 1, according to $hv_o = k\theta_D$ (h is the Plank's constant) [24]. To determine v_o for the different compositions, the Debye temperature θ_D was estimated by $T > \theta_D/2$ (Eq. 3). θ_D of the present glasses was obtained to be 711–729 K, which was nearly the same as the values of V_2O_5–P_2O_5 [25] Thus, these estimated θ_D values indicate to be physically reasonable. Then, with the θ_D values, v_o was calculated using $v_o = k\theta_D/h$. The values of θ_D and v_o are summarized in Tables 1 and 2. The values of small polaron coupling constant γ_p, a measure of electron–phonon interaction, given by the formula $\gamma_p = 2W_H/hv_o$ [16, 20] were also evaluated for the present glasses. The estimated value of γ_p is 9.35–17.44 (Table 2), which is larger than those for V_2O_5–Bi_2O_3 glasses doped with $BaTiO_3$ (7.05–7.60) [26] and less than Fe_2O_3–$Na_2P_2O_6$ glasses (66.74–97.60) [27]. The value of $\gamma_p > 4$ usually indicates a strong electron–phonon interaction [15] (Figs. 4, 5).

The hopping carrier mobility μ can be estimated for the present glasses. For non-adiabatic hopping regime, μ is given by [28]:

$$\mu = \left(\frac{eR^2}{kT}\right)\left(\frac{1}{h}\right)\left(\frac{\pi}{4W_H kT}\right)^{1/2} J^2 \exp\left(\frac{-W}{kT}\right). \quad (10)$$

μ values were estimated for $T = 300$ K with the data of R, J, and W_H in Tables 1 and 2. The hopping carrier concentration N_c is then obtained using the well-known formula $N_c = \sigma/e\mu$. Table 3 shows the results, indicating that

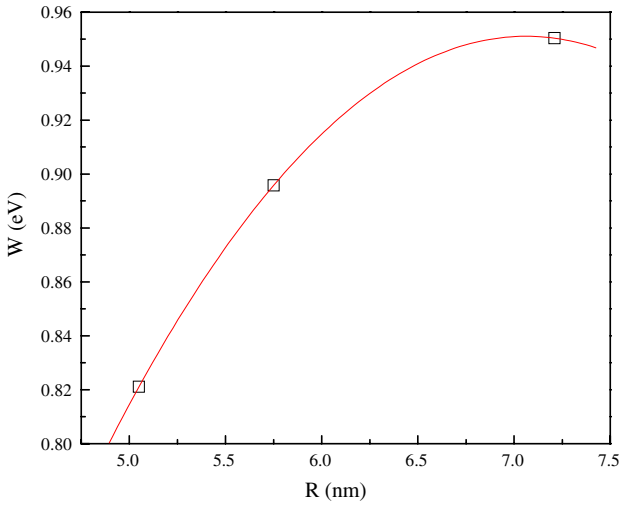

Fig. 4 Effect of the mean distance (R) on activation energy (W) for different glass compositions

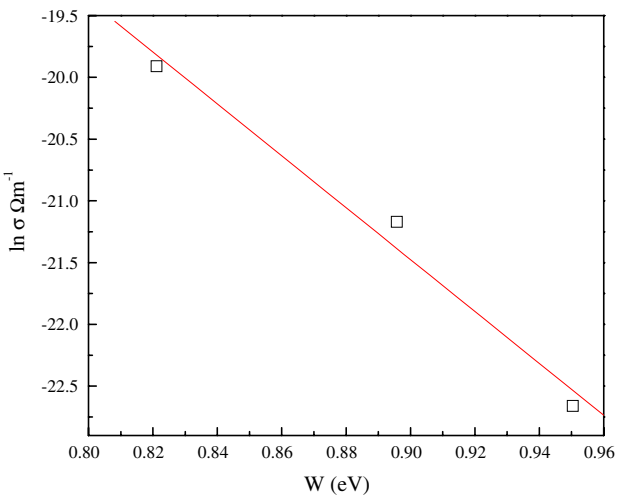

Fig. 5 Effect of activation energy (W) on dc conductivity (ln σ) at $T = 300$ K for different glass compositions ($\tan\theta = -1/2.303$ kT)

Table 3 Hopping carrier mobility and density of Bi_2O_3–PbO–Fe_2O_3 glasses

Glass no.	μ ($cm^2\ V^{-1}\ S^{-1}$)	$N_c \times 10^{21}$ (c^{-3})
1	8.128×10^{-13}	11.02
2	2.569×10^{-11}	0.155
3	4.963×10^{-9}	0.0028

the μ increases with Fe_2O_3 content. μ values were evaluated to be 8.12×10^{-11}–4.96×10^{-7} $cm^2\ V^{-1}\ s^{-1}$ and N_c values 11.02×10^{21}–0.28×1019 cm^{-3}, being the same order as those for NiO–V_2O_5–TeO_2 glasses [29]. As the localization condition for hopping electrons is $\mu > 10^{-2}$ $cm^2\ V^{-1}\ S^{-1}$ [28], the results mean that electrons in the present glasses are localized mainly at iron site. Therefore, conduction in the present glasses is due to hopping [30].

Figure 6a, b, showed the variation of dielectric constant, ε', and dielectric loss, ε'', with temperature, for the sample containing 10 mol.% Fe_2O_3, as a representing example of the present glass system. It can be noticed that, the values of ε' and ε'' decreases with increase in frequency and increases with increase in temperature. Similar results were observed in all samples. These measured ε' values of the present glasses are in agreement with the reported ε' values for similar glass systems containing transition metal oxides [31].

The increase in dielectric constant of the sample with increase in temperature is usually associated with the decrease in bond energies [5]. That is, as the temperature increases two effects on the dipolar polarization may occur; (i) it weakens the intermolecular forces and hence enhances the orientation vibration, (ii) it increases the thermal agitation and hence strongly disturbs the orientation vibrations. The dielectric constant becomes larger at lower frequencies and at higher temperatures, which is normal in oxide glasses and, is not an indication for spontaneous polarization [2]. This may be due to the fact that as the frequency increases, the polarizability contribution from ionic and orientation sources decreases and finally disappear due to the inertia of the ions.

In Fig. 6a, b, it can be seen that the ε' increases with increase in temperature and at high temperatures it increases more rapidly. This behavior is typical to the polar dielectrics in which the orientation of dipoles is facilitated with rising temperature and thereby the dielectric constant is increased. At low temperatures, the contribution of electronic and ionic components to the total polarizability will be small. As the temperature is increased, the electronic and ionic polarizability sources start to increase [8].

On the other hand, Fig. 7 shows the permittivity at room temperature as a function of composition and frequency, it can be noted that the dielectric constant, ε', increases with

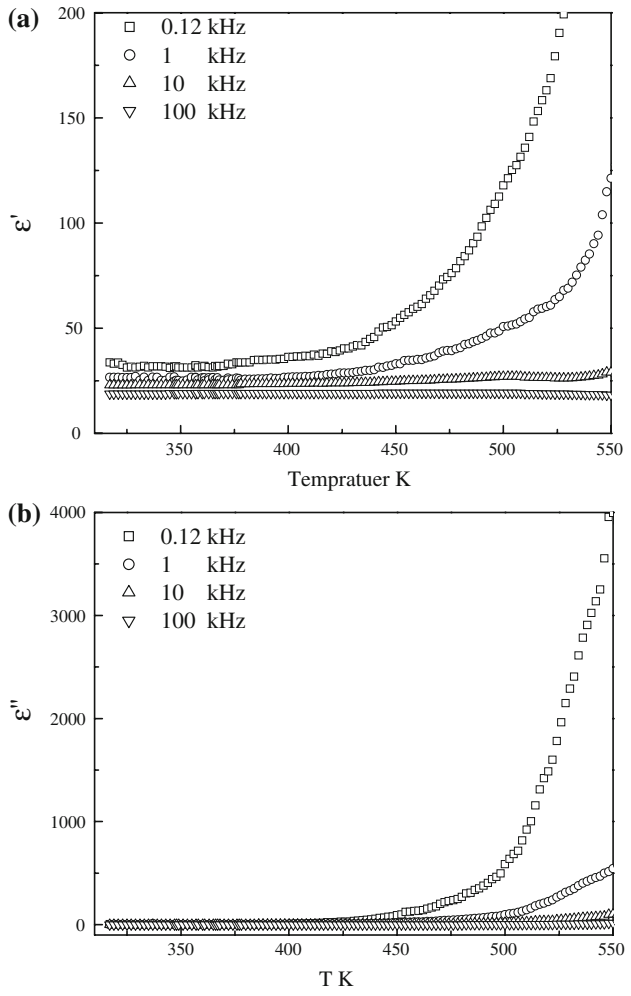

Fig. 6 A representative example of the dielectric permittivity as a function of temperature for a glass sample with $x = 10$ mol.% Fe_2O_3

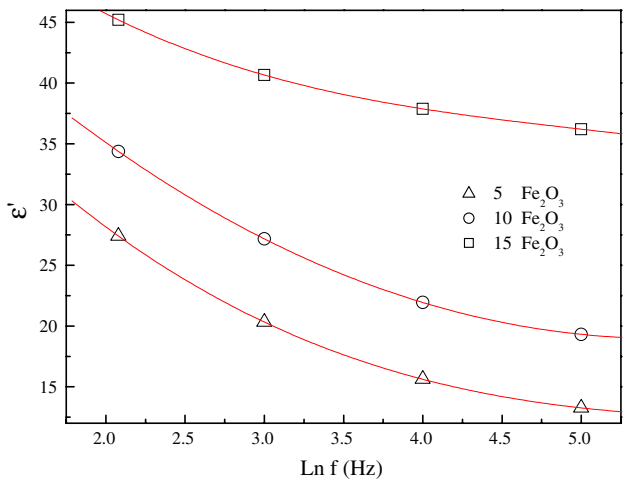

Fig. 7 Dielectric permittivity as function of glass composition and frequency at room temperature for the glass system $(80 - x)Bi_2O_3$–$20PbO$–xFe_2O_3 where $x = 5$, 10, and 15 mol.%

increase in Fe_2O_3 concentration in the glass system. It may be attributed to the decrease in electronic contribution to the total polarizability [3, 7].

The frequency dependent conductivity $\sigma_{ac}(\omega)$ increases approximately linearly with angular frequency ω:

$$\sigma_{ac}(\omega) = \sigma_t(\omega) - \sigma_{dc} = A\omega^S, \tag{11}$$

where the frequency exponent $S \leq 1$, and $\sigma_t(\omega)$ is the total conductivity, which is actually the measured factor in an ac experiment. The experimental value of the measured ac conductivity as a function of temperature and frequency are shown in Fig. 8 for a glass of the composition containing 10 mol.% Fe_2O_3 as an example of the glass series, other compositions of the series show similar behavior. The phenomenon has previously been attributed to relaxation caused by the motion of electrons, atoms, hopping or tunneling between the equilibrium sites [15].

The frequency dependence of conductivity suggests the hopping conductivity. The S values were calculated from the slopes of $Ln\sigma_{ac}$ versus Lnf plots. The estimated frequency exponent S is shown in Fig. 9 as a function of temperature from room temperature onwards. The exponent S decreases smoothly with increasing temperature. The numerical values of S at room temperature are in the range $0.85 < S < 0.98$, which are closely associated with proven carrier transport: hopping electrons. It has been established that a value of S close to unity is to be associated with the lattice responses [32]. The distinction between lattice and carrier responses is that they correspond to intrinsic and extrinsic processes, respectively, due to some impurities or injected carriers as a result of the existence of transition metal ions.

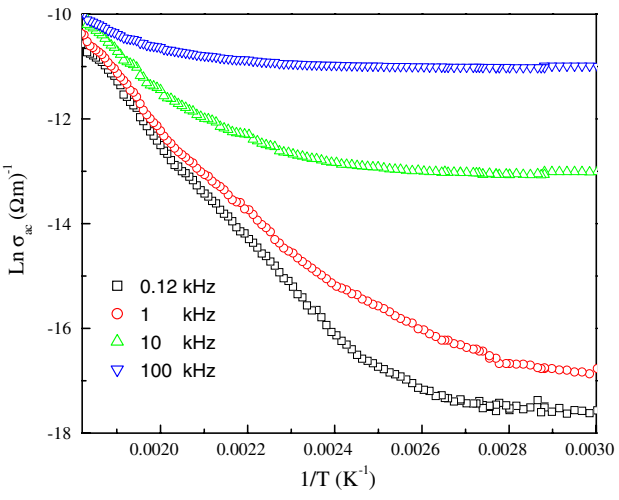

Fig. 8 A representative example of ac electrical conductivity as a function of temperature and frequency, for a glass with $x = 10$ mol.% Fe_2O_3. All other samples show similar behavior in the frequency range 0.12–100 kHz

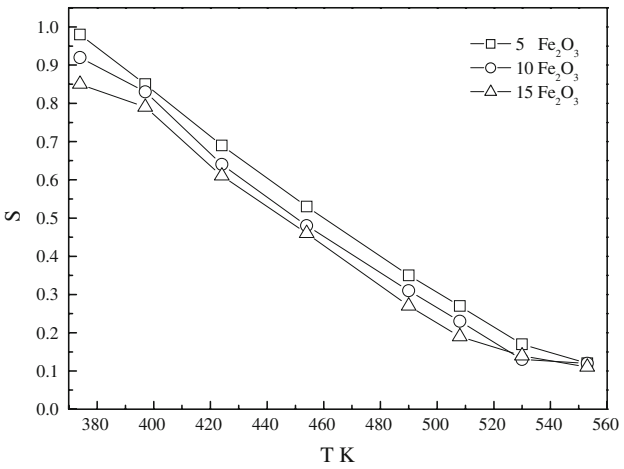

Fig. 9 Plot of the frequency exponent, S, as a function of temperature, for the glass system $(80 - x)Bi_2O_3$–$20PbO$–xFe_2O_3 where $x = 5$, 10, and 15 mol.%

On the other hand, the complex dielectric constant is represented by $\varepsilon^* = \varepsilon' + j\varepsilon''$, where ε' is the real part and ε'' the imaginary part of the dielectric permittivity, respectively. And, the corresponding real part of the ac conductivity obeys the following relation:

$$\sigma_{ac}(\omega) = \varepsilon_o \omega \varepsilon' \tan\delta, \tag{12}$$

where $\tan\delta = \varepsilon''/\varepsilon'$, defines the loss tangent, which is independent of the sample geometry, ε_o is the free space permittivity. According to Elliott [32], the correlated barrier hopping (CBH) model was proposed and was applied to the chalcogenide glassy semiconductors as well as to oxide glasses. In this model, the bipolaron has been proposed to interpret the frequency dependent conductivity. This model was successful in explaining many temperature dependent conductivity results at low temperature. However, it does not explain the high temperature behavior particularly in the low frequency range. This theory was extended to high temperature by assuming a single polaron hopping [33], where it produces more satisfactory results. In this respect, the ac conductivity of Eq. 12 may be given for correlated narrow-band limit for random sites and single polaron hopping [34] as:

$$\sigma_{ac}(\omega) = \frac{1}{24}\pi^3 \varepsilon_o \varepsilon' \omega \left(\frac{R_\omega}{R}\right)^6, \tag{13}$$

where $R = (1/N)^{1/3}$, as given above, while the hopping distance R_ω at frequency ω is given by;

$$R_\omega = \frac{e^2}{\pi \varepsilon_o \varepsilon' [W_M - KT\ln(1/\omega\tau_o)]}, \tag{14}$$

where e is the electronic charge, ε' the dielectric constant, ε_o the dielectric constant of free space, W_M the maximum barrier height, τ_o the Debye relaxation time of the order

Table 4 Electrical parameters of Bi_2O_3–PbO–Fe_2O_3 glasses

Glass no.	W_M (eV)	W_{ac} (eV)	$\frac{R_\omega}{R}$	R_ω (Å)	S	ln σ_o $(\Omega\ m)^{-1}$
1	0.712	0.7891	1.11	1.79	0.98	5.17
2	0.558	0.760	1.21	3.00	0.92	4.89
3	0.446	0.735	1.38	4.71	0.85	4.72

10^{-13} s [15, 31], and K the Boltzmann constant. On applying Eq. 13 to the experimental ac conductivity data, it was found that the factor (R_ω/R) is in the range (1.11−1.38 Å) as a function of composition and frequency for the present system, see Table 4 These results indicate a hopping distance R_ω (1.79−4.71 Å), up to 300 K, using the permittivity data when the exponent S, is active, i.e., for frequencies above 1.0 kHz, see Fig. 7. Table 4 collects the obtained results. On the contrary, the frequency dependent conductivity in the CBH model can be expressed in terms of the frequency exponent S, of Eq. 11 as:

$$S = 1 - \frac{6KT}{W_M - KT\ln(1/\omega\tau_o)}. \quad (15)$$

On the other hand, in the CBH model, electrons in charged defect states would hop over the coulombic barrier of height W, given as;

$$W = W_M - \frac{ye^2}{\pi\varepsilon_o\varepsilon R}, \quad (16)$$

where y is the number of electrons to hop ($y = 1$ for single polaron case and $y = 2$ for the bipolaron case), and e the electronic charge. In this respect, we may use the familiar notation for the relaxation time as given by [34, 35]:

$$W = KT\ln(1/\omega\tau_o). \quad (17)$$

The experimental data of the frequency exponent S, as a function of temperature, shown in Fig. 9 of the glass system $(80 - x)Bi_2O_3$–20PbO–xFe_2O_3, where $x = 5$, 10 and 15 mol.%, it is noted that the S values decrease with temperature. This suggests that the CBH conductivity is dominant in ac conductivity mechanism of the present glass system.

Conclusion

Semiconducting $(80 - x)Bi_2O_3$–20PbO–xFe_2O_3, where $x = 5$, 10 and 15 mol.%, glasses were prepared by the press-quenching technique from the melts. The XRD curves confirm the amorphous nature of the present samples. The dc conduction mechanics was investigated in terms of different physical models. The inverse temperature dependence of log(σ) in the range 300–550 K gave linearity but deviated from linearity for temperatures less than about 400 K. The conduction of the present glasses was confirmed to be due to primarily non-adiabatic hopping of small polaron between Fe^{2+} and Fe^{3+} ions in the glass network, this corresponded to relatively small polaron coupling constants ($\gamma_p = 2.45$–3.52). The dielectric constant, ε', increases with increase in Fe_2O_3 concentration in the glass system. It may be attributed to the decrease in electronic contribution to the total polarizability. The frequency exponent S decreases as the temperature increases, which suggests that the CBH conductivity is dominant in ac conductivity mechanism of the present glass system.

References

1. Hall D, Newhause N, Borrelli N, Dumbaugh W, Weidman D (1998) J Appl Phys Lett 54:1293
2. Sankarappa T, Prashant Kumar M, Devidas GB, Nagaraja N, Ramakrishnareddy R (2008) J Mol Struct 889:308
3. Shaaban MH, Ali AA, El-Nimr LK (2006) J Mater Chem Phys 96:423
4. Iordanova R, Dimitriev Y, Kassabov S, Klissurski D (1996) J Non-Cryst Solids 204:141
5. Bahgat AA, Abou-Zeid YM (2001) J Phys Chem Glasses 42:01
6. Bentley FF, Smithson LD, Rozek AL (1968) Infrared-spectra and characteristic frequencies. Interscience, New York, p 103
7. Venkateswara Rao P, Satyanarayana T, Srinivasa Reddy M, Gandhi Y, Veeraiah N (2008) J Phys B 403:3751
8. Mogus-Milankovic A, Licina V, Reis ST, Day DE (2007) J Non-Cryst Solids 353:2659
9. Lines ME, Miller AE, Nassau K, Lyons KB (1987) J Non-Cryst Solids 89:163
10. Durga DK, Veeraiah N (2002) Phys B 324:127
11. Srinivasarao G, Veeraiah N (2002) J Phys Chem Solids 63:705
12. Rajendran V, Palanivelu N, Chaudhuri BK, Goswami K (2003) J Non-Cryst Solids 320:195
13. Rusu D, Ardelean I (2008) J Mater Res Bull 43:1724
14. El-Desoky MM, Al-Shahrani A (2006) J Phys B 383:163
15. Mott NF, Davis EA (1979) Electronic processes in non-crystalline materials, 2nd edn. Clarendon Press, Oxford
16. Austin IG, Mott NF (1969) Adv Phys 18:41
17. Chung CH, Mackenzie JD (1980) J Non-Cryst Solids 42:357
18. Sayer M, Mansingh A (1972) Phys Rev B 6:4629
19. Dhawan VK, Mansingh A, Sayer M (1982) J Non-Cryst Solids 51:87
20. Mott NF (1968) J Non-Cryst Solids 1:1
21. Holstein T (1959) Ann Phys (NY) 8:325
22. EL-Desoky MM, Tashtoush NM, Habib MH (2005) J Mater Sci Mater Electron 16:533
23. Bogomolov VN, Kudinov EK, Firsov YA (1968) Sov Phys Solid State 9:2502
24. Meckenzie JD (1966) Vitreous state encyclopedia physics. Reinhold, New York, p 769
25. Field MB (1969) J Appl Phys 40:2628
26. Chakrabaty S, Sadhukhan M, Modak DK, Chaudhuri BK (1995) J Mater Sci 30:5139. doi:10.1007/BF00356061
27. Al-Shahrani A, El-Desoky MM (2006) J Mater Sci Mater Electron 17:43
28. Murawski L, Chung CH, Mackenzie JD (1979) J Non-Cryst Solids 32:91

29. El-Desoky MM (2003) J Mater Sci Mater Electron 14:215
30. El-Desoky MM (2005) J Non-Cryst Solids 351:3139
31. Bahgat AA, El-Samanoudy MM, Sabry AI, Phys J (1999) Chem Solids 60:1921
32. Elliott SR (1990) Physics of amorphous materials, 2nd edn. Longman, London
33. Shimakawa K (1982) Phil Mag B 46:123 see also p 48, 77
34. Elliott SR (1987) Adv Phys 36:135
35. Bahgat AA (1998) J Non-Cryst Solids 226:155